JOURNAL OF Materials CHEMISTRY

The photoelectrochemical study of a series of ionically combined bischromophore transition metal complexes in LB films

Jin Zhai,[a] Tian-Xin Wei,[b] Chun-Hui Huang*[b] and Hong Cao[b]

[a]*Laboratory of Organic Solids, Institute of Chemistry, Chinese Academy of Sciences, Beijing 100080, P.R. China*
[b]*State Key Laboratory of Rare Earth Materials Chemistry and Applications, Peking University, Beijing 100871, P.R. China. E-mail: hch@chemms.chem.pku.edu.cn*

Received 13th September 1999, Accepted 10th December 1999

Five transition metals were selected as the central ions to coordinate with 4,5-dimercapto-1,3-dithiole-2-thione to form five complex anions which were combined with hemicyanine dye to form five complexes, bis{[(*E*)-*N*-octadecyl-4-[2-(4-dimethylaminophenyl)ethenyl]pyridinium}bis(4,5-dimercapto-1,3-dithiole-2-thionato)metalate [$D_2M(dmit)_2$, where M = Ni, Pd, Cu, Cd, Hg]. Data show that $D_2Cd(dmit)_2$ is the best in terms of the photoelectric conversion among the five complexes. The quantum yield of $D_2Cd(dmit)_2$ is 5 times greater than that of (*E*)-*N*-octadecyl-4-[2-(4-dimethylaminophenyl)ethenyl]pyridinium iodide (DI) itself. UV-vis and fluorescent spectroscopy were used to characterize the compounds and study the interaction of the ions. A semiempirical quantum chemical calculation by PM3 was used to elucidate the role of the counter anions. By combining the experimental and theoretical results, it was found that the electronic configuration of the transition metals and the geometric configuration of the counter anion play important roles in the photoelectric conversion system.

Introduction

In the study of superconducting materials, complexes of a transition metal and the sulfur-containing ligand dmit (H_2dmit = 4,5-dimercapto-1,3-dithiole-2-thione) have been proposed to be good superconductors.[1] Hemicyanine dyes are a class of nonlinear optical materials well known for their large second-order molecular hyperpolarizabilities.[2] Recently, our group reported an investigation into the photoelectrochemical properties of a series of hemicyanine congeners, with quantum yields of about 0.22–0.50%.[3] The introduction of the complex anion $Zn(dmit)_2^{2-}$ to replace the iodide in hemicyanine was also studied, and it was found that this anion is quite effective for promoting photoelectric properties and second harmonic generation.[4,5] In this paper, five transition metals with d^8, d^9 and d^{10} electronic configurations were selected as central ions to coordinate with the ligand $(dmit)^{2-}$ to form five complexes. The structures of the complexes are shown below.

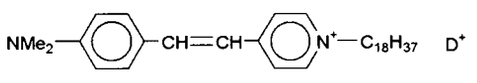

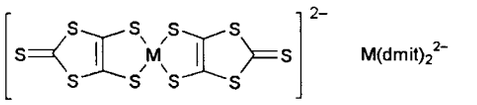

M = Ni, Pd, Cu, Cd, Hg

The photocurrent generation properties of the complexes were studied along with the UV-vis and fluorescence spectra of these complexes. A possible mechanism for the electron transfer process is proposed and the results from semiempirical quantum chemical calculation by PM3 are used to elucidate the roles of the different counterions with the same d^{10} electronic configuration in the charge transfer process.

Experimental

1 Materials

4-Dimethylaminobenzaldehyde, 1-iodooctadecane, 4-methylpyridine, tetrabutylammonium bromide, carbon disulfide and sodium metal were all A.R. grade products from Beijing Chemicals. The hydroquinone (HQ) was A.R. grade from Beijing Chemical Factory and was used as received. All the other chemicals were A.R. grade. The subphase was in-house deionized water purified by passing through a EASY-pure RF compact ultrapure water system (Barnstead Co., USA).

2 Synthesis

(1) The synthesis of bis(tetrabutylammonium) bis(4,5-dimercapto-1,3-dithiole-2-thionato)nickelate was performed following the procedures of Steimecke.[6] Compounds of the other four transition metals were synthesized following the same procedures.

(2) The synthesis and characterization of the hemicyanine dye and its complexes with 4,5-dimercapto-1,3-dithiole-2-thione containing different central atoms were performed by following the methods described in reference 7. The purification was carried out by recrystallizing the compounds three times from acetone. Elemental analysis results are as follows: $D_2Ni(dmit)_2$, found (calc.)%: C 62.18(61.76), H 7.87 (7.98), N 3.54 (3.89); $D_2Pd(dmit)_2$, found (calc.)%: C 58.12 (58.45), H 7.04 (7.02), N 3.84 (4.01); $D_2Cu(dmit)_2$, found (calc.)%: C 60.76 (61.29), H 7.44 (7.52), N 4.03 (3.97); $D_2Hg(dmit)_2$, found (calc.)%: C 55.85 (55.88), H 6.82 (6.85), N 3.51 (3.62); $D_2Cd(dmit)_2$, found (calc.)%: C 58.86 (59.26), H 7.24 (7.27), N 4.00 (3.84).

3 π–*A* Isotherm and film deposition

Langmuir–Blodgett (LB) films of each complex were formed by dropping a $CHCl_3$ (distilled) or CH_2Cl_2 (distilled) solution of the complex onto a pure water subphase (20 ± 1 °C, pH = 5.6) in a British NIMA Technology Langmuir–Blodgett Model 622

trough, leaving the solution for 10 min to allow evaporation of the solvent, and then compressing the complex layer at a rate of 40 cm^2 min^{-1}. The surface pressure–area (π–A) isotherm was recorded at this time. Transparent indium tin oxide (ITO) coated glass substrates with 200 Ω lateral resistance were cleaned and pretreated hydrophilicly according to the traditional procedure.[8] The LB films were fabricated by dipping the substrates into the aqueous subphase and raising them at a rate of 5 mm min^{-1} with a moderate surface pressure of 30 mN m^{-1}. The up transfer ratios were about 1.0 ± 0.1.

4 Spectroscopic measurements

The UV-vis spectra were recorded on a Shimadzu UV-3200 spectrometer (Japan). A Hitach-850 fluorescent spectrometer (Japan) was used to record the fluorescent spectra.

5 Photoelectrochemical measurements

A conventional three-electrode system was used in the photoelectrochemical experiments. The ITO glass coated with the LB film was used as the working electrode, with an effective irradiation area of 0.5 cm^2, with platinum wire as the counter electrode and a saturated calomel electrode (SCE) as the reference electrode. 0.1 mol L^{-1} KCl was used as the supporting electrolyte for all the electronic measurements. The modified electrodes were irradiated with a 500 W xenon lamp (Ushio Electric). All measurements were carried out at room temperature on a Model 600 Voltammetric Analyzer (CH Instruments, USA). Different wavelengths were obtained by using various filters with a certain bandpass (Toshiba KL-40 ~ KL-80). The intensity of the incident beams was checked by a power and energy meter (Model 372, Scientech). The IR light was filtered throughout the experiments with a Toshiba IRA-25S filter (Japan) to protect the electrodes from heat.

Results and discussion

1 π–A isotherms

Fig. 1 shows the π–A isotherms of the complexes. All the complexes have a phase transition in their solid state regions implying that molecular reorientation may take place at the air–water interface (shown in the inset in Fig. 1). Table 1 shows the parameters of the LB films. The limiting areas of $D_2M(dmit)_2$ (0.80–0.90 nm^2) are nearly twice as large as that of DI (0.50 nm^2) at the same surface pressure (30 mN m^{-1}), while the collapse pressures differ only slightly.

Table 1 The parameters of the π–A isotherms of the $D_2M(dmit)_2$ complexes

	Limiting area/nm^2	Collapse pressure/mN m^{-1}
$D_2Ni(dmit)_2$	0.80	55
$D_2Pd(dmit)_2$	0.80	43
$D_2Cu(dmit)_2$	0.90	45
$D_2Cd(dmit)_2$	0.85	40
$D_2Hg(dmit)_2$	0.85	40
DI	0.50	44

2 UV-Vis spectroscopic characterization

The maximum absorption peaks of the five title complexes both in DMF solution and as LB films are shown in Table 2.

From the UV-vis spectra of $(Bu_4N)_2M(dmit)_2$, $Ni(dmit)_2^{2-}$ has three absorption peaks. One of them is in the UV region, corresponding to the π–π* transition. The peak at 633 nm can be assigned to the d–d transition of the central metal atom. The peak at 418 nm is assigned to the d–p interaction because the d orbitals of the central metal ion interact with the p orbitals on the two ethylene double bonds through the lone-pair electrons on the four sulfur atoms, and the π orbitals on the ethylene double bonds then interact with the π orbitals on the thiocarbonyl groups through the lone-pair electrons on the outer four sulfur atoms.[9] For $Cu(dmit)_2^{2-}$, the d–d transition is quite weak so no peak is observed around 600 nm, the peak at 542 nm represents the d–p interaction while the peak at 404 nm is assigned to an n–π* transition. As for $Cd(dmit)_2^{2-}$, since the electron configuration of Cd^{2+} is d^{10} the d–d transition disappears, and the only peak in the visible region of 480 nm can be assigned to the d–p interaction. The two peaks in the UV region can be assigned to π–π* and n–π* transitions. The mercury complex is very similar to that of cadmium because they are in the same group.

The UV-vis spectra of the LB monolayers of the five complexes show broad charge-transfer absorption bands with maxima ranging from 464 to 485 nm, which are all blue shifted by about 10 nm compared with their DMF solutions.

3 Photoelectric conversion properties of LB film modified electrodes

Steady cathodic photocurrents were observed when the complex modified ITO electrodes were irradiated with white light (200 mW cm^{-2}). The cathodic photocurrent indicates that the electrons flow from the electrode through the LB film to the electrolyte solution.

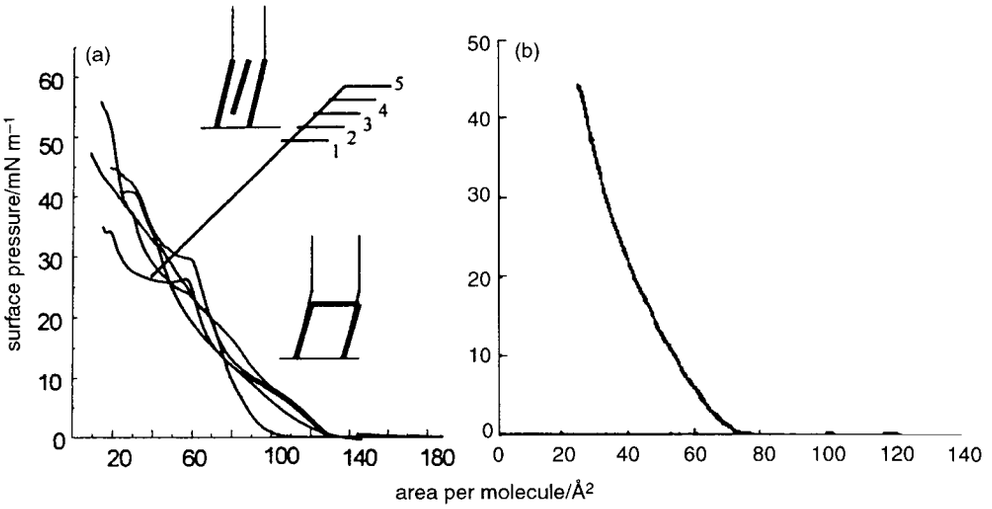

Fig. 1 The π–A isotherms of the complexes at the air–water interface. a: 1, $D_2Cd(dmit)_2$. 2, $D_2Ni(dmit)_2$. 3, $D_2Pd(dmit)_2$. 4, $D_2Hg(dmit)_2$. 5, $D_2Cu(dmit)_2$. b: DI. Inset: The possible arrangement of the cation D^+ and the counteranion $Cd(dmit)_2^{2-}$ in LB films on the ITO.

Table 2 UV-vis spectral absorption peaks of the complexes in DMF solution and in LB films[a]

	Maximum absorption/nm	
Complex	DMF(10^5 ε/dm^3 mol^{-1} cm^{-1})	LB film
$D_2Cd(dmit)_2$	480 (1.4)	464.5
$D_2Ni(dmit)_2$	486 (0.63)	485
$D_2Pd(dmit)_2$	503 (in CH_2Cl_2 solution)	468.5
$D_2Cu(dmit)_2$	476 (1.6)	468.5
$D_2Hg(dmit)_2$	479 (0.75)	480
$(NBu_4)_2Cd(dmit)_2$	504 (0.2), 315 (0.3), 293 (0.3)	
$(NBu_4)_2Ni(dmit)_2$	633 (0.059), 418 (0.1), 316 (0.27)	
$(NBu_4)_2Cu(dmit)_2$	542 (0.13), 404 (0.12)	
$(NBu_4)_2Hg(dmit)_2$	509 (0.22), 320 (0.32)	
DI	473 (0.3)	

[a]The concentrations of the complexes are 1×10^{-5} mol L^{-1} while that of DI is 2.1×10^{-5} mol L^{-1}.

As an example, the action spectrum of the $D_2Cd(dmit)_2$ modified electrode is shown in Fig. 2. The action spectra data of the five complex modified electrodes are listed in Table 3. The data show that the most effective wavelength is 464 nm for all the complexes, coinciding with the absorption of the LB films, indicating that the complexes in LB films are responsible for the photocurrent generation. The quantum yields and the photocurrents of the five complexes are listed in Table 4. It is very interesting that the complex of $D_2Cd(dmit)_2$ is the best in terms of photocurrent generation.

4 Factors affecting $D_2M(dmit)_2$ modified ITO electrodes

Fig. 3 shows the relationship between the photocurrents and the bias potentials of the five complexes. The cathodic photocurrents increased with increasing negative bias potential and *vice versa*. From this figure, the open circuit photovoltages of the five compounds can be obtained. They are 300, 188, 166, 191, 241 mV for $D_2Cd(dmit)_2$, $D_2Hg(dmit)_2$, $D_2Cu(dmit)_2$, $D_2Ni(dmit)_2$ and $D_2Pd(dmit)_2$ respectively, and once again the $D_2Cd(dmit)_2$ complex has the greatest value, reflecting that it has the greatest LUMO energy level among the five complexes. (The open circuit voltage is related to the energy level of the excited state and the energy level of the acceptors in the solution. Because the experiments were carried out under the same conditions, the open circuit voltages in this system are related to the energy level of the dyes' excited state.)

Fig. 4 shows the effects of the electron donor HQ on the photocurrent. The photocurrents decreased when HQ was added. The effects of nitrogen and oxygen on the photocurrent generation were examined at the same time. Nitrogen can decrease the cathodic photocurrent while subsequently oxygen may recover the photocurrent at the beginning of the oxygen bubbling process. Normally oxygen is regarded as an electron acceptor since it can accept an electron to form a superoxide anion. As expected, the donor (HQ) decreases the cathodic photocurrent while the acceptor (O_2) enhances the cathodic photocurrent.

Fig. 5 shows the relationship between the light intensity and the photocurrent generation. According to Donoan,[10] the photocurrent generated, i, is dependent on the irradiation light intensity, I, according to $i=kI^m$, where $m=1$ is characteristic of unimolecular recombination and $m=1/2$ is characteristic of bimolecular recombination. From Fig. 5, it can be seen that the m values of the four complexes are all approximately equal to 1. So the separated charge loss process occurring in this system is unimolecular recombination.

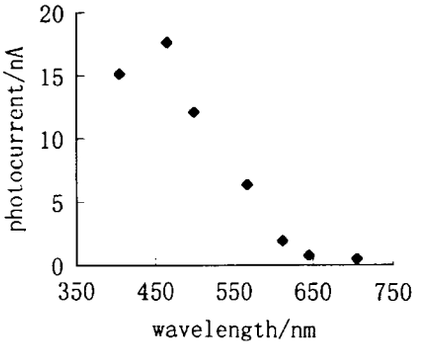

Fig. 2 The action spectrum of $D_2Cd(dmit)_2$. Irradiation with the white light of 200 mW cm^{-2} in a 0.1 mol L^{-1} KCl electrolyte solution. The effective irradiation area is 0.5 cm^2. The intensities of different wavelengths were all normalized.

5 Possible mechanism

a UV-visible and fluorescent spectra study. As an example, Fig. 6 shows the UV-vis spectra in DMF solution of hemicyanine, $D_2Cd(dmit)_2$, $(NBu_4)_2Cd(dmit)_2$ and the overlay of the spectra of hemicyanine and $(NBu_4)_2Cd(dmit)_2$. It is evident that the UV-vis spectrum of the overlay of hemicyanine and $(NBu_4)_2Cd(dmit)_2$ spectra coincides well with that of $D_2Cd(dmit)_2$ after normalization at the maximum absorption. This phenomenon indicates that there is no interaction between the hemicyanine cation and $Cd(dmit)_2^{2-}$ anion at the ground state, but the increase in the value of ε implies that the transition moment of the compound $D_2Cd(dmit)_2$ is increased and its dipole moment is increased as well.

The peak of the emission fluorescent spectrum of hemicyanine appeared at 640 nm when 450 nm light was used to excite the sample. When a small amount of a DMF solution of $(NBu_4)_2M(dmit)_2$ was added to the bulk solution of DI, the emission of DI decreased. This fluorescent quenching phenomenon implies that in the five systems hemicyanine and the counter anion $M(dmit)_2^{2-}$ interact at the excited state. According to the Stern–Volmer formula:

$$F_0/F = 1 + K_{sv}[Q]$$

where F_0 and F are the fluorescent intensities when the concentrations of the quenching agent are zero and $[Q]$ respectively. When F_0/F is plotted against $[Q]$, a linear relationship between them and consequently the quenching constant K_{sv} can be found. Table 5 shows the K_{sv} values of the corresponding compounds. From the absorption spectra and the quenching of the fluorescent spectra, it can be concluded that dynamic fluorescent quenching occurs in this system and

Table 3 Photocurrent generation of monolayer film modified ITO electrodes under irradiation with different wavelengths[a]

	Photocurrent/nA			
Wavelength/nm	$D_2Ni(dmit)_2$	$D_2Cu(dmit)_2$	$D_2Pd(dmit)_2$	$D_2Hg(dmit)_2$
404	8.677	4.88	3.688	16.21
464	15.15	5.76	4.303	18.47
498	10.178	4.25	3.336	13.13
567	3.898	1.44	1.265	5.58

[a]The intensities of different wavelengths were all normalized.

Table 4 Photocurrents and quantum yields of monolayer film modified electrodes

Complex	Quantum yield (%)	Photocurrent/nA cm^{-2} [b]
$D_2Ni(dmit)_2$	0.309	600–1200
$D_2Pd(dmit)_2$	0.12	600–900
$D_2Cu(dmit)_2$	0.12	800–1160
$D_2Zn(dmit)_2$[a]	0.68	1200
$D_2Cd(dmit)_2$	1.1	1600–1984
$D_2Hg(dmit)_2$	0.5	1400–2426
hemicyanine[a]	0.22	300–356

[a]Quoted from references 3 and 5. [b]Irradiated with white light of 200 mW cm^{-2} in a 0.1 mol L^{-1} KCl electrolyte solution.

the charge-transfer complex may be formed at the excited states.[11] Since there is no overlap between the emission spectrum of DI and the absorption spectrum of each $(NBu_4)_2M(dmit)_2$, the fluorescent quenching is mainly led by charge transfer, not by energy transfer. The order of quenching constants of these five $(NBu_4)_2M(dmit)_2$ complexes is: $(NBu_4)_2Ni(dmit)_2 > (NBu_4)_2Cu(dmit)_2 > (NBu_4)_2Zn(dmit)_2 > (NBu_4)_2Cd(dmit)_2 > (NBu_4)_2Hg(dmit)_2$.

There is another form of the Stern–Volmer formula:

$$\frac{\tau_0}{\tau} = 1 + K_{sv}[Q]$$

where τ_0 and τ are the fluorescent lifetimes when the concentrations of the quenching agent are zero and $[Q]$ respectively. Considering the excited state lifetime, the greater the quenching constant, the shorter is the excited state lifetime. It is feasible that a long-lived excited state will enhance the production of the charge separate state and hence generate a greater photoelectric current. So the compounds containing Zn, Cd and Hg (d^{10} metals) have better photocurrent generation properties than the other compounds.

According to all these photoelectric experiments, the UV-vis spectra and the fluorescent spectra, the possible electron transfer mechanisms are proposed in Scheme 1.

When the compound $D_2M(dmit)_2$ is irradiated, the cation, D^+, is excited to become $[D_2{}^*M(dmit)_2]$. The electrons may flow from $[D_2{}^*M(dmit)_2]$ to the electrolyte solution while $[D_2M(dmit)_2]$ accepts an electron from the electrode, so that the whole process is that an electron flows from the electrode and passes through the LB film to the electrolyte solution to form a cathodic photocurrent.

b The effect of the counter anion structure on the photoelectric conversion. Because the compounds of $D_2M(dmit)_2$ have the same cation, the only difference between them is the central atom in the counter anion, so the structures of the counter anions become more important in the promotion of the photoelectric conversion. In order to understand this phenomenon, a single crystal of $(NBu_4)_2Cd(dmit)_2$ was synthesized.[12]

In the counter anion, cadmium is coordinated with the sp^3 hybrid orbitals and the configuration is distorted tetrahedral, differing from those of nickel and copper which are in a planar configuration.[13] Data show that the planar configuration with larger conjugation in $Ni(dmit)_2^{2-}$ and $Cu(dmit)_2^{2-}$ is not as good as the tetrahedral configuration with smaller conjugation in $Zn(dmit)_2^{2-}$ and $Cd(dmit)_2^{2-}$ for photocurrent generation in

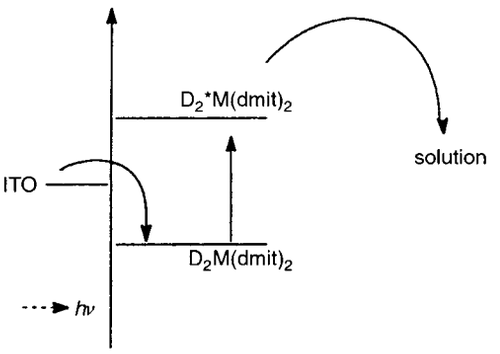

Scheme 1 The possible mechanism of the photoelectric conversion systems.

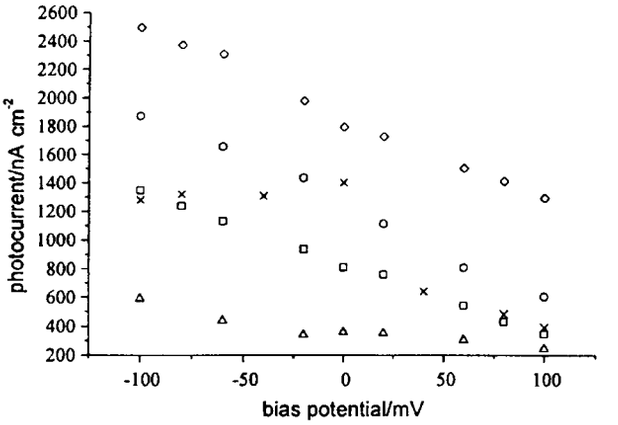

Fig. 3 The effect of the bias potential on the photocurrent generation. Irradiation with white light of 200 mW cm^{-2} in a 0.1 mol L^{-1} KCl electrolyte solution. ◇ $D_2Cd(dmit)_2$, □ $D_2Cu(dmit)_2$, × $D_2Ni(dmit)_2$, △ $D_2Pd(dmit)_2$, ○ $D_2Hg(dmit)_2$.

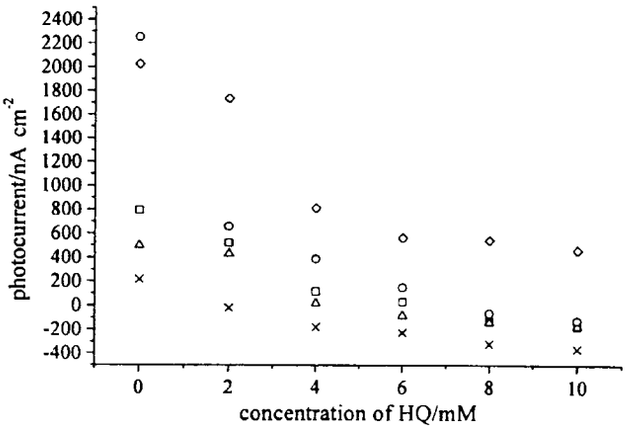

Fig. 4 The effect of the electron donor (HQ) on the photocurrent generation. Irradiation using white light of 200 mW cm^{-2} in a 0.1 mol L^{-1} KCl electrolyte solution. ◇ $D_2Cd(dmit)_2$, □ $D_2Cu(dmit)_2$, × $D_2Ni(dmit)_2$, △ $D_2Pd(dmit)_2$, ○ $D_2Hg(dmit)_2$.

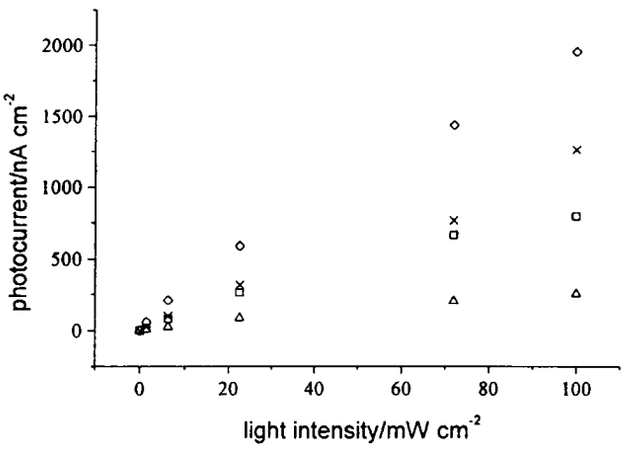

Fig. 5 The relationship between the light intensity and the photocurrent generation. Irradiation with white light in a 0.1 mol L^{-1} KCl electrolyte solution. ◇ $D_2Cd(dmit)_2$, □ $D_2Cu(dmit)_2$, × $D_2Ni(dmit)_2$, △ $D_2Pd(dmit)_2$.

Table 5 The quenching constants K_{sv} of the complexes $D_2M(dmit)_2$

	K_{sv} ($\times 10^5$)	R^a
$(NBu_4)_2Ni(dmit)_2$	0.06	0.9
$(NBu_4)_2Cu(dmit)_2$	0.04	0.9
$(NBu_4)_2Zn(dmit)_2$	0.02	0.9
$(NBu_4)_2Cd(dmit)_2$	0.01	0.9
$(NBu_4)_2Hg(dmit)_2$	0.01	0.9

[a]The linear correlation coefficient.

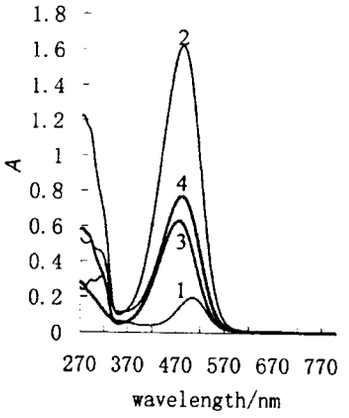

Fig. 6 The UV-vis spectra of 1 $(NBu_4)_2Cd(dmit)_2$, 2 $D_2Cd(dmit)_2$, 3 DI and 4 the overlay of spectra 1 and 3 in DMF solution. The concentrations of 1, 2, 3 are 1.1×10^{-5}, 1.0×10^{-5} and 2.1×10^{-5} mol L^{-1} DMF solutions respectively.

the $D_2M(dmit)_2$ system. One reason for this is that as a spacer between the two chromophores, the metal D^+ helps to keep the chromophores separate more effectively because the tetrahedral configuration of the counter anions has a larger volume. This will benefit the charge separation of the cation D^+.[12] Another reason is that the smaller conjugation extent in the tetrahedral configuration is favorable for charge separation and consequently favorable for photocurrent generation in this system.

c A semiempirical quantum chemical calculation. Cadmium and zinc have the same electronic configuration, d^{10}, and the same tetrahedron coordination configuration. So why is $Cd(dmit)_2^{2-}$ better than $Zn(dmit)_2^{2-}$ in photoelectric conversion? To better understand this phenomenon, PM3 including configuration interaction (C.I. = 4) in the MOPAC program package was used to calculate the compositions of the HOMO and LUMO orbitals, and the dipole moments at the ground state and the first excited state, of the cadmium and zinc species. The crystal data of $Cd(dmit)_2^{2-}$ [12] and $Zn(dmit)_2^{2-}$ [14] were used in the calculation.

The labelling model is shown in Scheme 2. From the eigenvectors and the eigenvalues, the atoms and orbitals that comprise the HOMO and LUMO orbitals are shown in Table 6. The data show that the difference in composition of the HOMO and LUMO orbitals for $Zn(dmit)_2^{2-}$ is quite large, while the difference for $Cd(dmit)_2^{2-}$ is relatively small. Table 7 shows the dipole moments at the ground state (μ_g) and the first excited state (μ_e) and the difference ($\Delta\mu$) for the complex anions. $\Delta\mu$ for $Cd(dmit)_2^{2-}$ is small while that for $Zn(dmit)_2^{2-}$ is large. From all these results, a smaller conjugation extent for

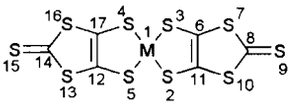

Scheme 2 The labeling model of $Cd(dmit)_2^{2-}$ and $Zn(dmit)_2^{2-}$ for theoretical calculations.

Table 7 The dipole moments at the ground state μ_g, the first excited state μ_e and the difference between them ($\Delta\mu$) for $Cd(dmit)_2^{2-}$ and $Zn(dmit)_2^{2-}$

	μ_g/D	μ_e/D	$\Delta\mu$ ($\mu_e-\mu_g$)/D
$Cd(dmit)_2^{2-}$	2.888	2.629	−0.259
$Zn(dmit)_2^{2-}$	4.744	0.861	−3.883

$Cd(dmit)_2^{2-}$ than for $Zn(dmit)_2^{2-}$ is deduced. Because the geometric configurations of $Cd(dmit)_2^{2-}$ and $Zn(dmit)_2^{2-}$ are both tetrahedral, the directions of their dipole moment are along the C_2 axis. As mentioned in reference 15, the dipolar–dipolar interaction of the chromophores is restrained by the large zinc complex anion. So, considering the influence of the spacer and the arrangement of the molecules in the LB films (see Fig. 1), interactions of the dipoles between anions and cations occur. If the dipole moments (μ_g, μ_e) and the difference between the ground state and the excited state ($\Delta\mu$) are quite large in the counter anion, the dipole interaction may lead to a decrease of the dipole moment of the cation and consequently will influence the charge separation of D^+. So small dipole moments (μ_g, μ_e) and a small dipole moment difference ($\Delta\mu$) between the ground and excited states of $Cd(dmit)_2^{2-}$ are favorable factors for the photoelectric conversion.

Conclusion

Photoelectric conversion properties of a series of transition metal complexes have been studied. The d^{10} metal containing complexes are better than d^8 and d^9 metal containing complexes in this aspect. The complex of $D_2Cd(dmit)_2$ is the best of those studied; the quantum yield is five times that of DI itself. This effect can be understood from the following aspects. (1) These complexes are a series of charge transfer complexes. The charge transfer process happens at the excited state but not at the ground state. The long-lived excited state enhances the charge separation. (2) Comparing the metals with d^8, d^9 and d^{10} electronic configurations, the complexes $D_2Zn(dmit)_2$, $D_2Cd(dmit)_2$, $D_2Hg(dmit)_2$ are better than $D_2Ni(dmit)_2$, $D_2Pd(dmit)_2$, $D_2Cu(dmit)_2$ in the photoelectric conversion. Since the coordination polyhedra of these two series of complexes are different, the former (with a smaller conjugation extent) lead to longer excited state lifetimes. (3) Quantum chemistry calculations indicate that smaller dipole moments (μ_g, μ_e) and a small dipole moment difference ($\Delta\mu$) between the ground and excited state are favourable for photoelectric conversion. We believe these results may shed light on the design of new photoelectroactive materials.

Acknowledgements

The authors thank the State Key Program for Basic Research (G1998061310), National Nature Science Foundation of China

Table 6 The orbitals of the labelled atoms which comprise the HOMO and LUMO orbitals

	HOMO	LUMO
$Cd(dmit)_2^{2-}$	$2(p_z)$, $3(p_z)$, $10(p_z)$, $6(p_z)$, $11(p_z)$, $9(p_z)$, $4(p_x, p_y)$, $12(p_x, p_y)$	$2(p_z)$, $3(p_z)$, $6(p_z)$, $11(p_z)$, $9(p_z)$, $4(p_x, p_y)$, $12(p_x, p_y)$, $5(p_x, p_y)$
$Zn(dmit)_2^{2-}$	$3(p_z)$, $5(p_x, p_y)$, $11(p_z)$, $12(p_x, p_y)$, $15(p_x, p_y)$, $16(p_x, p_y)$, $17(p_x, p_y)$	$2(p_z)$, $3(p_z)$, $4(p_z, p_y)$, $5(p_x, p_z)$, $6(p_z)$, $11(p_z)$

and Fund for Doctoral Student for financial support of this work.

References

1 R. A. Clark, *The Physics and Chemistry of Organic Superconductors*, Springer Verlag, Berlin, 1990.
2 G. J. Ashwell, R. C. Hargreaves and C. E. Baldwin, *Nature*, 1992, **357**, 393.
3 A. D. Lang, J. Zhai, C. H. Huang, L. B. Gan, Y. L. Zhao, D. J. Zhou and Z. D. Chen, *J. Phys. Chem. B*, 1998, **102**(8), 1424.
4 W. S. Xia, C. H. Huang, L. B. Gan and H. Li, *J. Chem. Soc., Faraday Trans.*, 1996, **92**, 3131.
5 W. S. Xia, C. H. Huang and D. J. Zhou, *Langmuir*, 1997, **13**, 80.
6 G. Steimecke, *Phosphorus Sulfur*, 1979, **7**, 49.
7 H. Li, D. J. Zhou and C. H. Huang, *J. Chem. Soc., Faraday Trans.*, 1996, **92**, 2585.
8 D. J. Zhou, C. H. Huang and H. Li, *Solid State Commun.*, 1996, **99**(10), 739.
9 S. G. Liu, P. J. Wu, Y. F. Li and D. B. Zhu, *Phosphorus Sulfur Silicon Relat. Elem.*, 1994, **90**, 219.
10 K. J. Donoan, R. V. Sudiwala and E. G. Wilson, *Mol. Cryst. Liq. Cryst.*, 1991, **194**, 337.
11 G. Q. Chen, *The Method of the Fluorescent Analysis*, Science Press, Beijing, 1990.
12 J. Zhai, C. H. Huang, T. X. Wei and H. Cao, *Polyhedron*, 1999, **18**, 1513.
13 O. Lindqvist, L. Sjolin, J. Sieler, G. Steimecke and E. Hoyer, *Acta Chem. Scand. A*, 1979, **33**, 445.
14 H. H. Wang, D. B. Zhu, X. Y. Zhu and H. Fu, *Acta Phys-Chim. Sin.*, 1985, **1**(4), 378.
15 D. J. Zhou, G. J. Ashwell and C. H. Huang, *Chem. Lett.*, 1997, 7.

Paper a907376k